Biochimica et Biophysica Acta 1857 (2016) 1917–1924

Contents lists available at ScienceDirect

Biochimica et Biophysica Acta

journal homepage: www.elsevier.com/locate/bbabio

Identification and characterization of multiple emissive species in aggregated minor antenna complexes

Md. Wahadoszamen [a,b,*], Erica Belgio [c,d], Md. Ashiqur Rahman [e], Anjue Mane Ara [f], Alexander V. Ruban [d], Rienk van Grondelle [a]

[a] Biophysics of Photosynthesis, Department of Physics and Astronomy, Faculty of Sciences, VU University Amsterdam, The Netherlands
[b] Department of Physics, University of Dhaka, Dhaka 1000, Bangladesh
[c] Institute of Microbiology, Academy of Sciences of the Czech Republic, Opatovický mlýn, 379 81 Třeboň, Czech Republic
[d] School of Biological and Chemical Sciences, Department of Cell and Molecular Biology, Queen Mary University of London
[e] Department of Physics, Khulna University of Engineering and Technology (KUET), Khulna 9203, Bangladesh
[f] Department of Physics, Jagannath University, Dhaka 1100, Bangladesh

ARTICLE INFO

Article history:
Received 17 June 2016
Received in revised form 10 September 2016
Accepted 21 September 2016
Available online 23 September 2016

Keywords:
Light harvesting
Minor antenna complexes
Photoprotective energy dissipation
Nonphotochemical quenching (NPQ)
Charge transfer states
Stark spectroscopy

ABSTRACT

Aggregation induced conformational change of light harvesting antenna complexes is believed to constitute one of the pathways through which photosynthetic organisms can safely dissipate the surplus of energy while exposed to saturating light. In this study, Stark fluorescence (SF) spectroscopy is applied to minor antenna complexes (CP24, CP26 and CP29) both in their light-harvesting and energy-dissipating states to trace and characterize different species generated upon energy dissipation through aggregation (in-vitro) induced conformational change. SF spectroscopy could identify three spectral species in the dissipative state of CP24, two in CP26 and only one in CP29. The comprehensive analysis of the SF spectra yielded different sets of molecular parameters for the multiple spectral species identified in CP24 or CP26, indicating the involvement of different pigments in their formation. Interestingly, a species giving emission around the 730 nm spectral region is found to form in both CP24 and CP26 following transition to the energy dissipative state, but not in CP29. The SF analyses revealed that the far red species has exceptionally large charge transfer (CT) character in the excited state. Moreover, the far red species was found to be formed invariably in both Zeaxanthin (Z)- and Violaxathin (V)-enriched CP24 and CP26 antennas with identical CT character but with larger emission yield in Z-enriched ones. This suggests that the carotenoid Z is not directly involved but only confers an allosteric effect on the formation of the far red species. Similar far red species with remarkably large CT character were also observed in the dissipative state of the major light harvesting antenna (LHCII) of plants [Wahadoszamen et al. PCCP, 2012], the fucoxanthin-chlorophyll protein (FCP) of brown algae [Wahadoszamen et al. BBA, 2014] and cyanobacterial IsiA [Wahadoszamen et al. BBA, 2015], thus pointing to identical sites and pigments active in the formation of the far red quenching species in different organisms.

© 2016 Elsevier B.V. All rights reserved.

1. Introduction

Photosynthesis is one of the most important physiological processes in nature, which enables photoautotrophs like green plants, algae and cyanobacteria to transform light energy into storable chemical energy. In doing so, the photosynthetic membrane of every photosynthetic organism is equipped with a variety of macromolecular protein complexes, specific lipids and highly conserved arrays of protein-bound chlorophyll (Chl) and carotenoid (Car) pigments [1,2]. The most abundant pigment-proteins in the thylakoid membrane of plants are the light-harvesting antenna complexes (LHCs), which attribute a central role in controlling the overall function of photosynthesis [3]. The key function of LHCs is to capture the available fraction of solar energy and transfer it efficiently and on an ultra-fast time scale to the reaction center where the solar-excitations are trapped to induce a stable transmembrane charge separation that drives the ensuing chemistry [4–6]. LHCs can also dissipate safely the excess photons harvested during intense sunlight and thereby protect the organisms from excess light induced highly toxic chemical by-products [7]. Therefore, photosynthetic organisms always encompass with a continuous paradox; in fact while light is the lifeblood for their growth and productivity, too much of it can potentially be lethal [8]. In order to cope and thrive with the deleterious effects of excess light plants, algae and some photosynthetic bacteria developed photoprotective mechanisms, via a concerted effort of several physiological processes collectively known as nonphotochemical

* Corresponding author at: Biophysics of Photosynthesis, Department of Physics and Astronomy, Faculty of Sciences, VU University Amsterdam, The Netherlands.
E-mail addresses: wahado.phy@du.ac.bd (M. Wahadoszamen), r.van.grondelle@vu.nl (R. van Grondelle).

http://dx.doi.org/10.1016/j.bbabio.2016.09.010
0005-2728/© 2016 Elsevier B.V. All rights reserved.

quenching (NPQ), which allow the harmless dissipation of the excess energy into heat [2,8–15]. Although the biological significance of NPQ is well established [11,16] the underlying molecular mechanisms associated with it are not clearly understood to date. In recent years a number of studies focused on unraveling the physical nature of the nonphotochemical quencher(s) in the light harvesting antenna of plants gave apparently contradictory results [14,15,17–25]. In fact, both Chl-Chl [22,25] and Chl-Car [17,18,20,26,27] interactions have been proposed to be responsible for energy dissipation. Yet, many physiological characteristics of NPQ have been found to be correlated positively with the formation of CT states in LHCs [17,18,22,25–29]. Although many studies point to the involvement of CT states (be it Chl-Chl or Chl-Car or both) in the excess energy dissipation through NPQ, very little is known about the underlying excited state electronic structures and the associated dynamics, the precise knowledge of which is essential not only for understanding NPQ on a molecular scale but also to design and develop robust artificial photosynthetic systems for efficient solar energy conversion.

An experimental technique that involves the perturbation of the molecular energy states by an externally applied electric field and the subsequent detection of spectral changes is known as the Stark spectroscopy. Stark spectroscopy is a very useful technique to trace and extract the electro-optic parameters such as change in permanent dipole moment and molecular polarizability associated with optical transitions of a photoactive species including those of photosynthetic pigment-protein complexes [30–35]. The determination of these parameters is central in characterizing the excited state electronic structure of a photoactive species under investigation. In particular, Stark spectroscopy is a very useful technique to trace and characterize mixed exciton-CT states because CT states are typically associated with a large electric dipole moment and thus exhibit a very sensitive response to the externally applied electric fields [32,33,36–39].

The artificial aggregation (quenching in-vitro) of light harvesting antennas of photosynthetic organisms is commonly considered to be the model system for the mimicry of NPQ as it occurs via excess light-induced conformational changes in vivo [40–43]. Formation of multiple emissive species is often found to be the consequence of artificial aggregation of light harvesting antennas [44]. Although, the signatures of multiple emissive species in an aggregated antenna can be diagnosed via conventional spectroscopies, but sometimes, because of overlapping spectral signatures, it is difficult to reveal their underlying excited state electronic structures and dynamics [35,37,38]. In addition, the efficiency of conventional spectroscopy is limited in tracing precisely the CT character of the states formed upon aggregation. The salient versatility of Stark spectroscopy offers the unique opportunity to resolve multiple overlapping spectral species and concomitantly reveals the underlying excited state electronic structure, dynamics, and a precise estimate about their CT character [35,45–47].

In our recent studies, we applied SF spectroscopy to the dissipative states of LHCII of higher plants [45], FCP of brown algae [46] and cyanobacterial IsiA [48]. We observed that the energy dissipation (in-vitro) in these pigment-proteins results in at least two emitting species, one of which has exceptionally large CT character. Minor antenna complexes (CP24, CP26 and CP29) are also believed to be directly involved in the NPQ process of higher plants [17,18,26,28,49–53]. However, it is not clear so far that, like for the major peripheral antenna LHCII, whether the energy dissipation in the minor antenna complexes is involved with the formation of multiple emitting species or not. If formed, what extent of CT character would they possess? Inter alias, it is suggested that the energy dissipation through minor antenna complexes is achieved predominantly via the interplay of CT state(s) [17,18,28,49,50,52,53]. In this regard, an unequivocal consensus on the carotenoid that is directly involved in the CT state formation is still lacking. In many studies, it is pointed out that Z is the carotenoid that forms the CT state [18,26,50,52,53], whereas, in some others, it is suggested that not Z but lutein (Lut) is involved in forming the CT state during the course of energy dissipation in minor antennas [17,28]. In the latter case, Z is suggested to attribute allosteric effects to the formation of the CT state. Keeping all the concerns in mind, in the present study, we applied SF spectroscopy to the minor light harvesting antenna complexes both in their light harvesting and in energy dissipating states to unravel:

(1) the number of emissive species generated upon formation of the energy dissipative state in each of these complexes.
(2) the electronic structures and excited state dynamics of all these species with a precise estimate of the CT character and the associated pigment compositions.
(3) how the formation yield of each species and its CT character is affected by the presence of the carotenoid Z (if Z is not directly involved in CT state formation).

2. Materials and methods

2.1. Isolation of PSII minor antenna complexes

Minor antenna complexes were isolated by isoelectric focusing of solubilized BBY particles prepared from spinach plants according to [54]. Plants were either dark adapted for 1 h or light treated for 45 min at 500 μmol m^{-2} s^{-1} under 98% N_2 flow to induce zeaxanthin formation. During BBY isolation of light-treated samples, a further incubation step of thylakoids with 40 mM ascorbate at pH 5.5 was performed to induce maximum violaxanthin de-epoxidation as described in [55].

2.2. Pigment analysis

Total pigments were extracted in 80% ice-cold acetone and centrifuged 5 min at max speed on a bench centrifuge. Total chlorophyll concentration and chlorophyll *a*/*b* ratios were calculated according to Porra et al. [56] from absorption at 646.6, 663.6, and 750 nm. Xanthophyll composition was determined by reversed-phase high-performance liquid chromatography using a LiChrospher 100 RP-18 column (Merck) connected with a Dionex Summit chromatography system as previously described [54].

2.3. Stark spectroscopy

5-fold quenched CP24/CP26/CP29 was obtained by incubation of the antenna with 50 mg of SM-2 Absorbent (Bio-Rad), allowing a 5-fold decrease in the fluorescence (F) intensity (i.e., the F intensity is decreased to 20%) upon aggregation. The sample for Stark spectroscopy of unquenched CP24/CP26/CP29 was prepared upon suspending it in a buffer containing 20 mM Hepes with pH-7.5, 20 mM NaCl, 10 mM $MgCl_2$, and 0.06% βDM and subsequent dilution with 60% (v/v) of glycerol for producing a transparent glass at 77 K. The preparation of the sample for Stark spectroscopy of the quenched CP24/CP26/CP29 was the same as for the unquenched samples, however in this case samples were devoid of the externally added detergent e.g. 0.06% βDM. SF spectroscopy was performed on the transparent frozen glasses of unquenched and quenched antennas at 77 K in a cell prepared upon gluing two glass slides, whose inner surfaces are coated with transparent layers of Indium Tin Oxide (ITO), with double-sided sticky tape (Sellotape). The optical path length of the resulting cell was 110 μm. The SF experiment was carried out on a homebuilt setup, similar to the one described in [34,45,46,48]. Briefly, the excitation wavelength was selected by dispersing the white light continuum of a Xenon lamp (Oriel) through a monochromator (1200 gmm grating blazed at 350 nm). The excitation beam hits the sample under an angle of 45°. The sample is immersed into the liquid N_2 chamber of an Oxford cryostat (DN1704) having strain free quartz optical windows. A low distortion sinusoidal AC voltage synthesized in the lock-in amplifier (SR850)

with modulation frequency of 80 Hz was applied to the sample after desired amplification through the high voltage generator. Both the F and SF signals were recorded simultaneously by the lock-in amplifier at the second harmonics of the modulation frequency. The details about the theoretical modeling of experimentally obtained SF data can be found elsewhere in the literature [31,34,46,48,57–60]. Briefly, the SF spectrum of randomly oriented and spatially fixed chromophores in a solid matrix (having negligible inter-chromophore interaction) can fairly be appreciated as the weighted superposition of the zeroth, first and second derivatives of the (field-free) F spectrum described by the following equation:

$$\frac{2\sqrt{2}\Delta F(\nu)}{F_{\max}} = (f\boldsymbol{F_{ext}})^2\left\{A_\chi F(\nu) + B_\chi \nu^3 \frac{d[F(\nu)/\nu^3]}{d\nu} + C_\chi \nu^3 \frac{d^2[F(\nu)/\nu^3]}{d\nu^2}\right\} \quad (1)$$

where $F_{\max}$ is the F intensity at the maximum, $\boldsymbol{F_{ext}}$ is the magnitude of the electric field applied externally during the course of experiment, ν is the energy in wavenumber, χ is the experimental angle between the direction of $\boldsymbol{F_{ext}}$ and the electric vector of the excitation light, and f is the local field correction factor used to estimate the magnitude of the internal electric field experienced by the chromophore(s), $\boldsymbol{F_{int}}$ via the relation $\boldsymbol{F_{int}} = f\boldsymbol{F_{ext}}$. The coefficient A_χ (denoted hereafter as zeroth derivative contribution, ZDC) reflects the field-induced change in emission intensity arising mostly from field-assisted modulation of the rates of nonradiative deactivations competing with the F process [34,35,57]. Besides, the coefficients B_χ and C_χ are associated with the electro-optic parameters, more specifically changes in molecular polarizability ($\Delta\alpha$) and molecular dipole moment ($\Delta\mu$) between the ground and excited states connected by the optical transition, respectively [34,35,57]. At the magic angle ($\chi = 54.7°$) the coefficients, B_χ and C_χ can be expressed as [34,57]:

$$B_{54.7°} = \frac{\Delta\alpha}{2\,hc} \quad (2)$$

$$C_{54.7°} = \frac{(\Delta\mu)^2}{6h^2c^2} \quad (3)$$

Therefore upon reproducing the SF spectrum by a weighted superposition of the derivatives of the corresponding F spectrum and computing the coefficients of the first and second derivatives, one can extract the values of $\Delta\alpha$ and $\Delta\mu$ from the above two equations. As the value of the local field correction f is not known, the values of $\Delta\alpha$ and $\Delta\mu$ in this study are expressed in terms of f. All the SF spectral fitting protocols of this study were performed using the commercially available Igor (WaveMetrics) software routine.

3. Results

Fig. 1 displays F (top) and SF (bottom) spectra of unquenched and 5-fold quenched CP24 (left panel), CP26 (middle panel), and CP29 (right panel) enriched with both V- and Z. Here and hereafter, the unquenched and 5-fold quenched samples of CP24/CP26/CP29 are denoted respectively as UQ-(V/Z)-CP24/UQ-(V/Z)-CP26/UQ-(V/Z)-CP29 and 5Q-(V/Z)-CP24/5Q-(V/Z)-CP26/5Q-(V/Z)-CP29, where V and Z stand for V- and Z-enriched samples, respectively. Both F and SF spectra are recorded simultaneously with excitation at 462 nm where the samples gave a negligible Stark absorption (SA) signal (see Fig. S1). The F spectra of both unquenched and quenched complexes in the figure are normalized to unity at their respective peaks, whereas the SF spectra are normalized to the field strength of 1 MV cm^{-1} and to the intensity at the peak of the respective F spectra. The F spectrum of all unquenched complexes is as usual featured by a characteristic sharp excitonic band with a peak at around 679–680 nm and a broad vibrational satellite with weak intensity peaking at around 740 nm (not shown here). On the other hand, the shapes of the F spectra of quenched complexes are notably different from the ones of the respective unquenched complexes. Distinct features of the F spectrum of a quenched complex include, among others, a strikingly broader emission lineshape with a major peak at around 685–695 nm and a broad tail stretching up to the end of the selected spectral window. In addition, in the case of quenched CP24 F, one can easily recognize the existence of an additional band in the 710–760 nm spectral region superimposed on the broad tail, the peak of which is located at around 730 nm. Interestingly, the far red band shows a more pronounced appearance with a well resolved lineshape in 5Q-Z-CP24 as compared with 5Q-V-CP24. On the contrary, such a far red emission band is not clearly distinguished in the F spectrum of the quenched CP26 and CP29 complexes. Indeed, both the 685–695 nm band of all quenched complexes and the 730 nm band of quenched CP24 originated as a consequence of the aggregation, and thus can be considered as the spectral signatures of some quenching species.

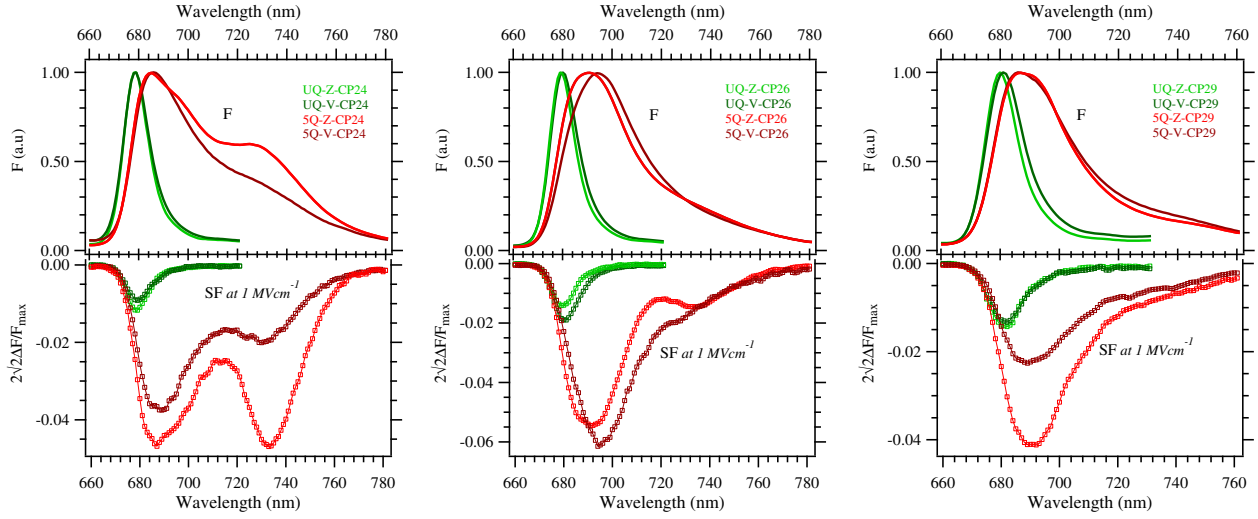

Fig. 1. F (top) and SF (bottom) of unquenched (light/dark green line) and 5-fold quenched (light/dark red line) of V/Z enriched CP24 (left panel), CP26 (middle panel) and CP29 (right panel) recorded simultaneously at 77 K. All the F spectra were normalized to unity at their maxima. To facilitate the estimation of electro-optic parameters, all the SF spectra are normalized to a field strength of 1 MV cm^{-1} and to the intensity at the peak of the respective F spectra.

Besides, regardless of the physical states of the antenna complexes (being either unquenched or 5-fold quenched), the SF spectra are characterized by negative amplitudes with shapes seemingly identical to the corresponding F spectra. The overall negative amplitude of the SF signal indicates that in all samples the externally applied electric field induces a fairly large reduction of F yield in combination with other expected electro-optic effects such as field-induced spectral shift and modification of the spectral bandwidth [45]. In addition, one can easily judge by glance that, albeit having (at least 5-fold) smaller F yield, all the quenched complexes gave (2–4 fold) larger relative SF intensity compared to their unquenched counterparts. This observation reflects the greater sensitivity of F states of the quenched antenna complexes to the external electric field. Furthermore, despite the fact that the signature of the far red band is weak in the F spectrum, it was prominently present with a well-defined lineshape in the SF spectrum. The intense appearance of the far red band in the SF spectrum is accompanied by a fairly large reduction of the bandwidth and a significant field-induced peak shift by about 5 nm to the red. It will be shown later that the reduced bandwidth and the notably large red-shifted peak of the SF signal of the far red band originate from the massive involvement of the electro-optic parameters $\Delta\mu$ and $\Delta\alpha$ of the associated species. Inter alia, although the far red band is barely resolved in the F spectrum of the quenched CP26, it gave a well resolved contribution to the SF spectrum especially of 5Q-Z-CP26. Once again, the intense appearance of 715–760 nm SF band is likely to be accompanied by a remarkably large magnitude of the field-induced peak shift and with the narrower bandwidth. However, in contrast to CP24 and CP26, the signature of such a far red band is neither observed in the F nor in the SF spectrum of the quenched CP29 complexes. In fact, the SF spectra of the quenched CP29 complexes seem to be virtually identical to the corresponding F spectra, whose peak is only shifted to the red by about 2–3 nm. Therefore it is very likely that a single quenching species is generated in CP29 following aggregation.

4. SF analyses

The analyses of the SF spectra of both unquenched and quenched samples of V/Z enriched CP24, CP26 and CP29 are performed by employing the Standard Liptay formalism as introduced above. In accordance with the Liptay formalism, the SF spectrum around a certain wavelength region can be reproduced (fitted) plausibly by the weighted superposition of the derivatives of the F spectrum provided that the F signal around that specific wavelength region arises from one type of non-interacting emissive species. Such an analysis would then yield a single set of molecular parameters (ZDC, $\Delta\alpha$ and $\Delta\mu$). On the other hand, if an F envelop contains emission contributions from multiple distinct species one cannot obtain a satisfactory fit of the corresponding SF spectrum only by the weighted superposition of the derivatives of the F spectrum as a whole. In such a case, the observed F spectrum needs to be deconvoluted into a set of bands representing the emission signatures of the available multiple species. The weighted sum of the derivatives of the deconvoluted bands can then be used to obtain a satisfactory fit of the SF spectrum. In such a case, one would obtain multiple distinct sets of molecular parameters associated with the decomposed bands. Therefore, by utilizing this unique feature of Stark spectroscopy one can simultaneously identify the number of emissive species present within the sample under study and compute precisely the corresponding molecular parameters, which in general cannot be done using conventional spectroscopy.

The SF spectrum of all unquenched minor antennas regardless of their reconstitution with V or Z could be well reproduced by the weighted superposition of the (zeroth, first and second) derivatives of the corresponding (field-free) F spectrum without deconvolution (see Fig. S2). The analysis thus yielded a single set of molecular parameters (ZDC, $\Delta\alpha$ and $\Delta\mu$) for all the unquenched complexes (see Table S1). This finding suggests that the F signal of each unquenched antenna complex arises from a single electronic state, which is the lowest excitonic state [61]. In addition, the very small magnitude of $\Delta\mu$ suggests that the only F state of each minor antenna complex has a weak CT character as anticipated.

In contrast to the case of unquenched complexes, the weighted superposition of the derivatives of the observed F spectra of both quenched CP24 and CP26 could not yield plausible fits of the corresponding SF spectra. In essence, the F spectrum of 5Q-Z-CP24 had to be deconvoluted into a minimum of three constituent bands peaking at 684, 707 and 731 nm as shown in Fig. 2a. The lineshape of each band was synthesized either by a single or a linear combination of some skewed Gaussians of varying FWHM and skewness. The weighted

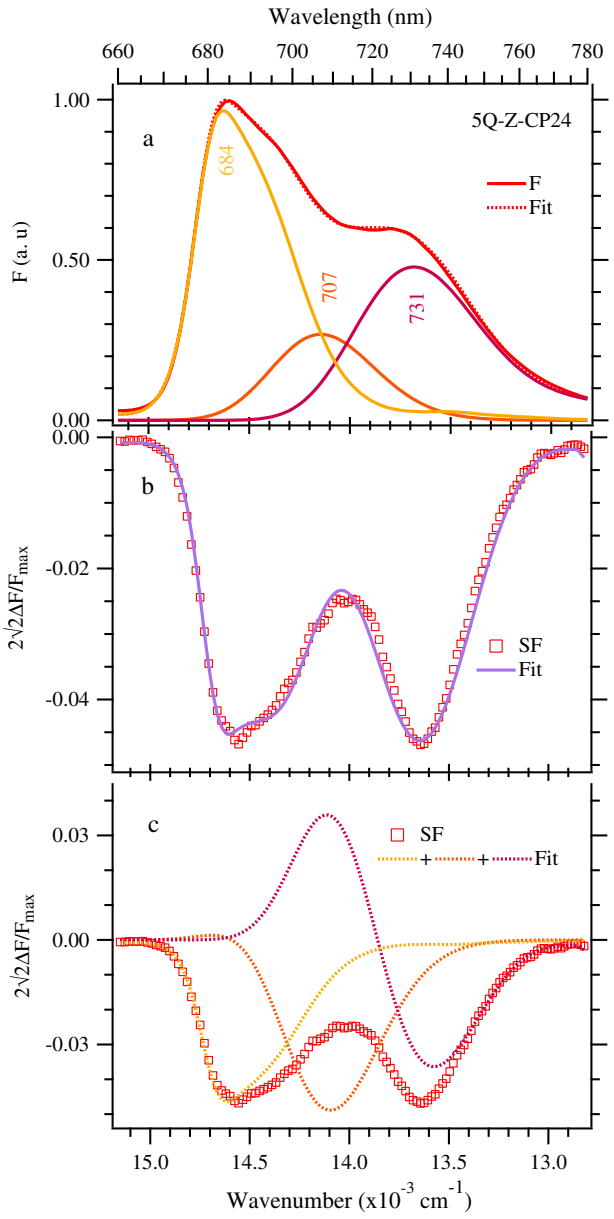

Fig. 2. (a) F (red solid line) spectrum of 5Q-Z-CP24 and the corresponding fit (red dashed line) obtained with linear superposition of some skewed Gaussians. The F spectrum is then deconvoluted into three constituent bands of varying skewness and width peaking at 684, 707 and 731 nm. The deconvolution is done in such a manner that they can yield plausible simultaneous fits of the F and SF spectra. (b) SF (red square-dotted line) spectrum and the resulting fit (light violet line) obtained with the weighted superposition of the derivatives of the deconvoluted bands. (c) SF spectrum (red square-dotted line) and the SF contributions (dashed lines) of the deconvoluted bands.

superposition of the derivatives of the deconvoluted bands was then used to reproduce the SF spectrum. Fig. 2b shows the resulting fit (light violet line) and Fig. 2c displays the SF contributions of the deconvoluted bands (dashed lines) together with the SF spectrum (red square-dotted lines). One can see (from Fig. 2c) that the SF contributions of the first two bands are seemingly identical in shape to the respective deconvoluted lineshapes and have strikingly large negative amplitudes. This finding suggests that the F yields of the species giving the two deconvoluted bands are highly reduced by the external electric field, thereby yielding the large magnitudes of the field induced reduction of F intensity (about 5–7% at 1 MV cm^{-1} field strength) as revealed by the large (negative) magnitudes of ZDC in modeling (see top part of Table 1). By applying a similar protocol, the SF spectrum of 5Q-V-CP24 could be fitted plausibly upon deconvoluting the F spectrum into three constituent bands peaking at 684, 707 and 732 nm (see Fig. S3). The ZDC and electro-optic parameters extracted from the two analyses are compiled in Table 1 (top part). One can see from the table that the analysis yielded very different sets of molecular parameters for each of the deconvoluted bands, indicating that they originate from emission of different excited electronic states. Alternatively, it can be said that the emission lineshapes of the deconvoluted bands are generated from different F species generated upon induction of quenching by aggregation in CP24. One may notice that the present analysis yielded a steady increase in Δμ values upon going from bluer to redder deconvoluted bands, indicating that the redder species attains much CT character compared to the bluer ones. Interestingly, the analysis yielded an exceptionally large value of Δμ for the red-most band of quenched CP24 that peaks around 730 nm spectral region, suggesting that the associated F state has a large CT character.

Unlike the case of quenched CP24, deconvolution of the F spectra of the quenched CP26 complexes into two constituent bands could yield acceptable simultaneous fits of the F and SF spectra. Fig. 3 illustrates the SF analysis of 5Q-Z-CP26. In this case, the observed F spectrum is deconvoluted into two bands of variable widths and skewness peaking at 690 and 733 nm, the weighted superposition of the derivatives of which simultaneously yielded a plausible fit (light violet line in Fig. 3b) of the SF spectrum throughout the wavelength region. Similarly, the SF spectrum of 5Q-V-CP26 could be fitted satisfactorily by deconvoluting the F spectrum into two bands (see Fig. S4). Middle part of Table 1 compiles the molecular parameters extracted from such analyses. Once again, the analyses yielded large magnitudes for Δμ of the far red band.

It is surprising that, unlike for quenched CP24 and CP26 complexes, the SF spectrum of quenched CP29 (both V and Z enriched) complexes could be reproduced well by just the weighted superposition of the derivatives of the observed F spectrum without deconvolution. Fig. 4 shows the resulting SF analyses of both 5Q-Z-CP29 (top panel) and 5Q-V-CP29 (bottom panel). The analysis eventually yielded a single set of molecular parameters (see bottom part of Table 1) for the both,

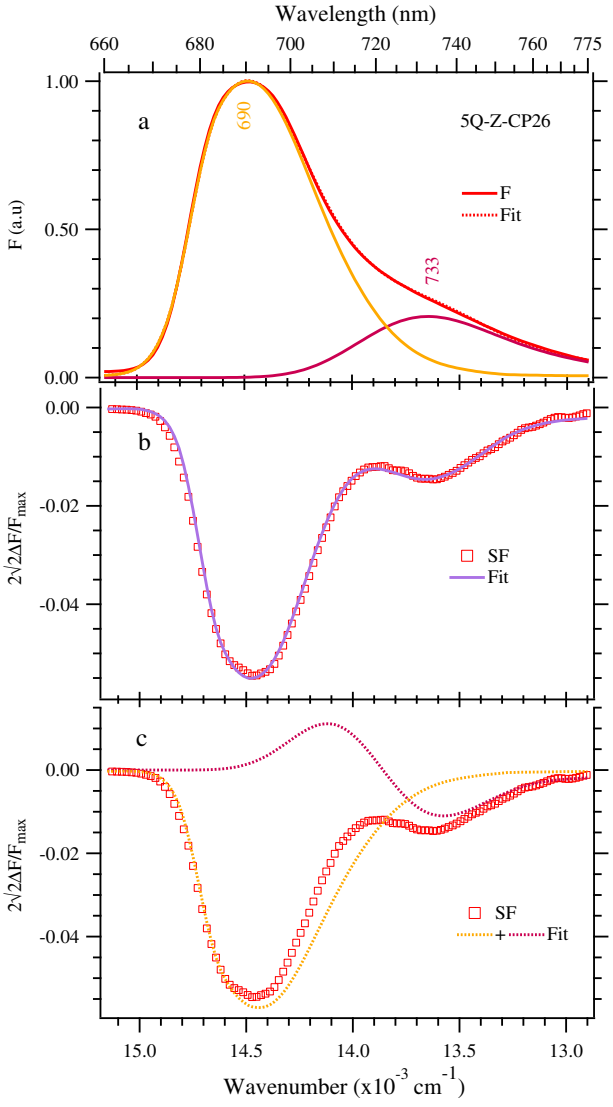

Fig. 3. (a) F (red solid line) spectrum of 5Q-Z-CP26 and the corresponding fit (red dashed line) obtained with linear superposition of some skewed Gaussians. The F spectrum is then deconvoluted into two constituent bands of varying skewness and width peaking at 690 and 733 nm. The deconvolution is done in a similar manner as in Fig. 2. (b) SF (red square-dotted line) spectrum and the resulting fit (light violet line) obtained with the weighted superposition of the derivatives of the deconvoluted bands. (c) SF spectrum (red square-dotted line) and the SF contributions (dashed lines) of the deconvoluted bands.

Table 1
Estimated molecular parameters from SF analyses of quenched samples.

Sample	Band	ZDC (at 1 MV cm^{-1})	Δα [$Å^3/f$]	Δμ [D/f]
5Q-Z-CP24	684	−0.047 ± 0.0012	−53.69 ± 6.11	0.80 ± 0.07
	707	−0.163 ± 0.0032	−429.5 ± 38.20	4.61 ± 0.37
	731	−0.012 ± 0.0026	−966.38 ± 36.21	10.31 ± 0.26
5Q-V-CP24	684	−0.04 ± 0.0005	−53.69 ± 3.49	1.13 ± 0.04
	707	−0.065 ± 0.0011	−178.96 ± 12.43	4.61 ± 0.11
	732	−0.01 ± 0.0004	−608.46 ± 16.66	10.31 ± 0.07
5Q-Z-CP26	690	−0.056 ± 0.0003	−89.48 ± 2.31	1.13 ± 0.09
	733	−0.01 ± 0.0011	−680.04 ± 25.45	9.79 ± 0.10
5Q-V-CP26	694	−0.065 ± 0005	−139.59 ± 5.70	0.65 ± 0.12
	732	−0.02 ± 0.0004	−680.04 ± 17.38	9.57 ± 0.14
5Q-Z-CP29	Single	−0.04 ± 0.0003	−71.58 ± 3.52	1.03 ± 0.07
5Q-V-CP29	Single	−0.022 ± 0.0002	−42.95 ± 1.50	0

indicating that a single F species is generated in CP29 following induction of artificial quenching. One can easily notice from Table 1 (bottom part) that the analysis yielded a fairly small magnitude of Δμ for 5Q-Z-CP29, zero Δμ for 5Q-V-CP29, indicating that the aggregation induced a single quenching species in CP29 complexes with little CT character like the unquenched counterparts and like all the 680–690 emissions of the other quenched complexes.

5. Discussion

By applying SF spectroscopy, we could identify multiple emissive species in the quenched aggregated CP24 and CP26 minor antennas. Three species giving emission peaks at around 680, 700 and 730 nm spectral regions are found to be formed in CP24, whereas two species giving emission peaks at 690–694 and 730 nm spectral regions are generated in CP26 following aggregation. The comprehensive modeling of the SF spectra employing standard Liptay formalism yielded small but

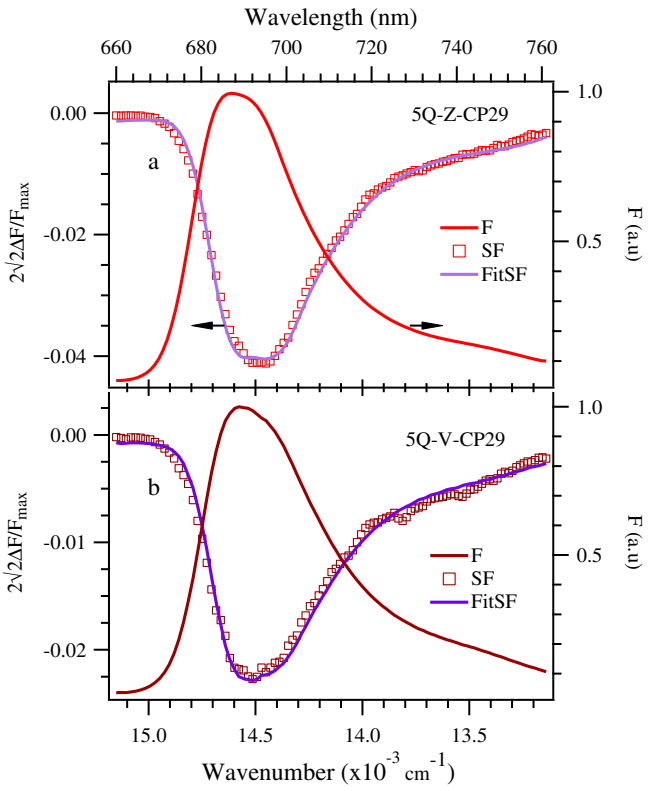

Fig. 4. a) F (red solid line), SF (red square-dotted line) and the fit (light violet line) of SF of 5Q-Z-CP29 obtained with the weighted superposition of the derivatives of the F spectrum without deconvolution. (b) F (deep red solid line), SF (deep red square-dotted line) and the Fit (violet line) of SF of 5Q-V-CP29 obtained with the weighted superposition of the derivatives of the F spectrum without deconvolution.

comparable magnitudes of Δμ for the first quenched species (responsible for the 684 and 690–694 emission bands in CP24 and CP26, respectively) and the respective unquenched counterparts (see Table S1). This suggests that a relatively small extent of charge separation and/or charge transfer exists among the excitonically coupled pigments of both the unquenched and first quenched species in their F states. In this respect, the comparable magnitude of Δμ suggests that the pigments involved with the charge separation and/or charge transfer are identical in both the unquenched and the first quenched species. Therefore, keeping a good analogy with unquenched emissive species [61], the first quenched emissive species of both CP24 and CP26 can be considered to originate predominantly from Chl-Chl interactions. Yet, the larger (negative) magnitude of Δα may reflect coarsely the larger extent of Chl-Chl interactions in this species resulting from the enhanced clustering of Chls pigments [62] within the modified local protein environment due to aggregation. To this end, the observed low F yield indicates that the aggregation-induced local protein environment confers a significantly large cross-section for nonradiative deactivation to this emissive species. The considerably larger negative ZDC then suggests that the rate of the nonradiative deactivation associated with the F state of the first quenched species is significantly enhanced by the externally applied electric field. Such an enhanced rate of non-radiative deactivation may occur when the cross-over to a nearby CT state constitutes one of the nonradiative deactivation pathways for this species. Therefore, like for the excitonically coupled bacteriochlorophyll dimers within an artificially prepared protein scaffold [57], the large cross-section for nonradiative deactivation of the first quenched species may result from the mixing of (Chl-Chl) excitonic state with an energetically nearby CT state. The extent of such mixing and thereby the rate of the nonradiative deactivation are highly enhanced by the externally applied electric field subsequently yielding a large (negative) amplitude of ZDC for this species. Due the involvement of a CT state in the nonradiative deactivation, clustering the Chls due to such aggregation induced modified local protein environment may potentially dissipate a large amount of excitation energy via a mechanism like concentration quenching [63,64] or open up a quenching channel to the Car [27], as aggregation is supposed to move the carotenoid (especially Lut) closer to the Chla cluster (and vice versa) within the terminal emitter domain. Similarly, by comparing the values of ZDC, Δα and Δμ with those obtained for the first quenched complexes of CP24 and CP26, we can assume that the only quenched emissive species of CP29 is generated from the enhanced Chl-Chl interaction upon aggregation. However, the SF analysis yielded nonzero magnitude of Δμ (1.03 [D]) for 5Q-Z-CP29 together with almost two times larger negative ZDC and Δα compared to 5Q-V-CP29 (which gave a zero Δμ). The larger magnitudes of the ZDC and electro-optic parameters may reflect the direct the involvement of Z in energy dissipation process in CP29.

The modeling of SF spectra yielded an extraordinarily large magnitude of Δμ for the 730 bands of both the quenched CP24 and CP26 complexes, indicating that the corresponding F states have exceptionally large CT character. Interestingly, not the extent of the CT character but the F yield of the associated species is found to be enhanced by the presence of the specific carotenoid Z. This suggests that, regardless of their xanthophyll composition, with either V or Z, a far red F species of identical CT character is formed in the aggregated CP24 and CP26: Z only gives allosteric effect to its emission yield. This also suggests that neither V nor Z is directly involved in the formation of the far red emissive species. Furthermore, the far red species of both the quenched complexes are very similar in terms of all the estimated molecular parameters (ZDC, Δα and Δμ), indicating that they are generated from the involvement of identical pigments interacting within similar sites surrounded by similar local protein environments in the two complexes. To this end, the strikingly large magnitude of Δμ indicates that the interacting pigments, among which the charge separation and/or charge dislocation exists, associated with the far red species are very different from those of the first quenched species. It is very likely that some Cars are involved along with Chls in yielding such an extraordinarily large magnitude of Δμ in the far red species. Note that Cars have a very large conjugated π skeleton characterized by a very strong excited intramolecular CT state [65]. Therefore, we can assume that the far red emissive species originates mainly from a closer Chl-Car interaction in the aggregated CP24 and CP26. It could also be possible that the aggregation induced far red band (of CP24/CP26) has the same origin as the 730 nm emission of native Lhca4, which is ascribed to a CT state originating from Chl-Chl interaction [39,66]. Note that the presence of an excitonically coupled Chl-Chl dimer is the characteristic feature of Lhca4. The dimer absorbs around 710 nm and subsequently gives the broad F band around 730 nm [67]. On the other hand, one can easily notice from Fig. S1 that both the unquenched and quenched complexes of all minor antenna gave identical SA lineshapes. This finding suggests that aggregation of any of the minor antenna complexes did not yield a Chl-Chl dimer (like for native Lhca4) or other ground state absorbing species by whose contribution the shape of SA spectrum would be modified. In this line of thinking, it is likely that the aggregation induced 730 nm band (of CP24/CP26) has an origin different from the far red bad of Lhca4. Inter alia, the appearance of the far red band is more noticeable in CP24 than in CP26, indicating that CP24 strongly favors the formation of the associated species. On the other hand, in sheer contrast to the cases of CP24 and CP26, such a far red emissive species is not formed in CP29 following artificial aggregation. Furthermore, the additional aggregation-induced species of CP24 that gives an emission peak at 707 nm gave several times larger/smaller Δα and Δμ values compared to the 684/730 species, indicating that the CT character of the corresponding F state is intermediate between the 685 and 730 states. However, from the fairly larger magnitude of Δμ we can assume that, like for the 730 species, Car interaction may also be associated with the formation of the 707 emissive species.

We could also identify multiple emissive species in the aggregated LHCII of higher plants [45], FCP of brown algae [46] and cyanobacterial IsiA [48]. In all the antennas, the artificial aggregation resulted in the formation of at least two emissive species associated with their quenched states, one gave an emission peak at around 690–695 nm region whereas the other gave the emission signature in the 730 nm region. From the comprehensive analyses of SF spectra, the 690–695 and 730 nm species of the aggregated LHCII, FCP and cyanobacterial IsiA were attributed to originate from Chl-Chl and Chl-Car interactions, respectively. However, due to having extremely low emission intensity, the signature of the far red band was not clearly resolved in the F spectrum of all the aggregated (LHCII, FCP, and cyanobacterial IsiA) samples. Therefore, the isolation of the far red emissive band (with appropriate width and position) was obtained from a number of simplifying assumptions and approximations. However, one can easily notice that the far red emission species of aggregated minor antenna complexes (especially of 5Q-Z-CP24) gives a clearly resolved and distinct bandshape with a peak around 730 nm. This in turn gives a good support that the peak selection of the far red band of aggregated LHCII and FCP was rather appropriate albeit done with some simplifying assumptions. The far red emission bands of the aggregated LHCII, FCP and cyanobacterial IsiA were assumed to originate from the interaction of Chls with Lut1, fucoxanthin, and echinenone in the terminal emitter locus, respectively. From the very good sequence homology with LHCII, we can also infer that the far red emissive species of the CP24 and CP26 originate from the interaction of Chls and Lut 1 in the terminal emitter domain. Luteins are suggested to form quenching channels in both major and minor light harvesting antennas [17,27]. From the transient absorbance analysis, Avenson et al. [17] proposed that two CT quenching channels constituted by Lut 1 and Z are present in CP26. The yield of CT quenching via the evolvement of Lut 1 was found to be enhanced considerably by the presence of Z in the L2 site. However, CT quenching through the involvement of Lut 1 was suggested to be absent in CP24 and CP29, where Z was considered to constitute the main CT quenching channel. Therefore, the absence of the far red emission band in CP29 is a direct manifestation that Lut 1 induced CT quenching is absent in this antenna in agreement with the proposal of Avenson et al. In contrast the presence of the far red emission band in CP24 is likely to be in contradiction with their proposal. Interestingly, SF analysis of all the minor antenna complexes (be they unquenched or quenched) yielded negative values of $\Delta\alpha$, which were in particular strikingly large for the far red emissive species of aggregated CP24 and CP26. Note that $\Delta\alpha$ estimated from SF spectroscopy reflects the difference in polarizability between the relaxed fluorescence (excited) state and the corresponding ground state. Then the observed negative values of $\Delta\alpha$ suggest that the fluorescence state has less polarizability than the ground state, which is apparently an unusual expectation. However, for photosynthetic pigment-proteins, $\Delta\alpha$ extracted from SF spectroscopy may result from the complexity of the excited states involved. For instance, the relaxed F state can be quantum mechanically (QM) mixed with nearby CT state(s) (a common scenario for photosynthetic pigment-proteins) thereby generating a dense and hybrid excited manifold [68]. Therefore, once a photoactive pigment is placed to the hybrid excited manifold, there is a finite possibility that the polarizability of the photoactive pigment is distributed over the available states that are QM-mixed. Moreover, the QM mixing may allow the CT state to borrow a significant amount of polarizability from the relaxed F state of the pigment as a CT state has essentially no polarizability. If this is the case, obtaining a negative value of $\Delta\alpha$ from SF measurement would not be very unusual. The QM mixing may also allow the F state to gain larger CT character from the CT state and in such a case a larger value of $\Delta\mu$ would be obtained from SF measurement. In the ideal case, the loss of polarizability and gain of CT character of the state can mutually be correlated; the larger the extent of mixing, the bigger the negative value of $\Delta\alpha$ and the bigger the magnitude of $\Delta\mu$ [68]. In this line of thinking, the negative value of $\Delta\alpha$ extracted from SF measurement can also be used as a marker that can assess the extent of the CT character of the associated F state. Then the large negative value of $\Delta\alpha$ for the far red species of both aggregated CP24 and CP26 strengthens the conclusion that their F states have stronger CT character. Interestingly, SF spectroscopy gave a negative polarizability change not only for most of the natural photosynthetic pigment- protein complexes we have studied so far [45,46,48] (in ref. 45 the absolute values of $\Delta\alpha$ were reported although they had negative sign) but also for the artificial photosynthetic pigment-protein complex [57], which we take as a strong indication for the mixing of CT states with the lowest exciton states in all these systems [68]. Finally, as the degree of CT character of a state is commonly inferred from the magnitude of $\Delta\mu$, a general conclusion can be drawn from the strikingly large magnitude of $\Delta\mu$ of the far red band that artificial aggregation generates a non-neutral longer wavelength state in most of the photosynthetic antenna complexes.

Transparency document

The Transparency document associated with this article can be found, in the online version.

Acknowledgement

Md. W., A. M. A., and R. v. G. were supported by the VU University Amsterdam, the Laserlab-Europe Consortium and the advanced investigator grant (267333, PHOTPROT) from the European Research Council. Md. W., and R. v. G. were supported further by the TOP grant (700.58.305) from the Foundation of Chemical Sciences part of NWO. A.V.R. was supported by the NWO visitors travel grant 040.11.433 to VU Amsterdam, Prof Rienk van Grondelle's laboratory.

Appendix A. Supplementary data

Supplementary data to this article can be found online at http://dx.doi.org/10.1016/j.bbabio.2016.09.010.

References

[1] J.F. Allen, J. Forsberg, Molecular recognition in thylakoid structure and function, Trends Plant Sci. 6 (2001) 317–326.
[2] J. Standfuss, A.C.T. van Scheltinga, M. Lamborghini, W. Kühlbrandt, Mechanisms of photoprotection and nonphotochemical quenching in pea light-harvesting complex at 2.5 Å resolution, EMBO J. 24 (2005) 919–928.
[3] A.R. Grossman, D. Bhaya, K.E. Apt, D.M. Kehoe, Light-harvesting complexes in oxygenic photosynthesis: diversity, control, and evolution, Annu. Rev. Genet. 29 (1995) 231–288.
[4] R. Vangrondelle, J.P. Dekker, T. Gillbro, V. Sundstrom, Energy-transfer and trapping in photosynthesis, Biochim. Biophys. Acta Bioenerg. 1187 (1994) 1–65.
[5] G.D. Scholes, G.R. Fleming, A. Olaya-Castro, R. van Grondelle, Lessons from nature about solar light harvesting, Nat. Chem. 3 (2011) 763–774.
[6] H. van Amerongen, J.P. Dekker, Light-harvesting in photosystem II, Light-Harvesting Antennas in Photosynthesis, Springer 2003, pp. 219–251.
[7] M.J. Davies, Reactive species formed on proteins exposed to singlet oxygen, Photochem. Photobiol. Sci. 3 (2004) 17–25.
[8] J. Barber, B. Andersson, Too much of a good thing — light can be bad for photosynthesis, Trends Biochem. Sci. 17 (1992) 61–66.
[9] P. Horton, A.V. Ruban, R.G. Walters, Regulation of light harvesting in green plants, Annu. Rev. Plant Physiol. Plant Mol. Biol. 47 (1996) 655–684.
[10] K.K. Niyogi, Photoprotection revisited: genetic and molecular approaches, Annu. Rev. Plant Physiol. Plant Mol. Biol. 50 (1999) 333–359.
[11] P. Muller, X.P. Li, K.K. Niyogi, Non-photochemical quenching. A response to excess light energy, Plant Physiol. 125 (2001) 1558–1566.
[12] C. Ilioaia, M.P. Johnson, P.N. Liao, A.A. Pascal, R. van Grondelle, P.J. Walla, A.V. Ruban, B. Robert, Photoprotection in plants involves a change in lutein 1 binding domain in the major light-harvesting complex of photosystem II, J. Biol. Chem. 286 (2011) 27247–27254.
[13] M.P. Johnson, M.L. Pérez-Bueno, A. Zia, P. Horton, A.V. Ruban, The zeaxanthin-independent and zeaxanthin-dependent qE components of nonphotochemical quenching involve common conformational changes within the photosystem II antenna in *Arabidopsis*, Plant Physiol. 149 (2009) 1061–1075.
[14] T.P. Krüger, C. Ilioaia, P. Horton, M.T. Alexandre, R. van Grondelle, How protein disorder controls non-photochemical fluorescence quenching, Non-photochemical Quenching and Energy Dissipation in Plants, Algae and Cyanobacteria, Springer 2014, pp. 157–185.

[15] L. Valkunas, J. Chmeliov, G. Trinkunas, C.D.P. Duffy, R. van Grondelle, A.V. Ruban, Excitation migration, quenching, and regulation of photosynthetic light harvesting in photosystem II, J. Phys. Chem. B 115 (2011) 9252–9260.
[16] A.V. Ruban, Nonphotochemical chlorophyll fluorescence quenching: mechanism and effectiveness in protecting plants from photodamage, Plant Physiol. 170 (2016) 1903–1916.
[17] T.J. Avenson, T.K. Ahn, K.K. Niyogi, M. Ballottari, R. Bassi, G.R. Fleming, Lutein can act as a switchable charge transfer quencher in the CP26 light-harvesting complex, J. Biol. Chem. 284 (2009) 2830–2835.
[18] T.J. Avenson, T.K. Ahn, D. Zigmantas, K.K. Niyogi, Z. Li, M. Ballottari, R. Bassi, G.R. Fleming, Zeaxanthin radical cation formation in minor light-harvesting complexes of higher plant antenna, J. Biol. Chem. 283 (2008) 3550–3558.
[19] S. Bode, C.C. Quentmeier, P.N. Liao, T. Barrosc, P.J. Walla, Xanthophyll-cycle dependence of the energy transfer between carotenoid dark states and chlorophylls in NPQ mutants of living plants and in LHC II, Chem. Phys. Lett. 450 (2008) 379–385.
[20] S. Bode, C.C. Quentmeier, P.N. Liao, N. Hafi, T. Barros, L. Wilk, F. Bittner, P.J. Walla, On the regulation of photosynthesis by excitonic interactions between carotenoids and chlorophylls, Proc. Natl. Acad. Sci. U. S. A. 106 (2009) 12311–12316.
[21] N.E. Holt, D. Zigmantas, L. Valkunas, X.P. Li, K.K. Niyogi, G.R. Fleming, Carotenoid cation formation and the regulation of photosynthetic light harvesting, Science 307 (2005) 433–436.
[22] A.R. Holzwarth, Y. Miloslavina, M. Nilkens, P. Jahns, Identification of two quenching sites active in the regulation of photosynthetic light-harvesting studied by time-resolved fluorescence, Chem. Phys. Lett. 483 (2009) 262–267.
[23] T.P.J. Kruger, V.I. Novoderezhkin, C. Ilioaia, R. van Grondelle, Fluorescence spectral dynamics of single LHCII Trimers, Biophys. J. 98 (2010) 3093–3101.
[24] P.N. Liao, C.P. Holleboom, L. Wilk, W. Kuhlbrandt, P.J. Walla, Correlation of Car S-1 → Chl with Chl → Car S-1 energy transfer supports the excitonic model in quenched light harvesting complex II, J. Phys. Chem. B 114 (2010) 15650–15655.
[25] Y. Miloslavina, A. Wehner, P.H. Lambrev, E. Wientjes, M. Reus, G. Garab, R. Croce, A.R. Holzwarth, Far-red fluorescence: a direct spectroscopic marker for LHCII oligomer formation in non-photochemical quenching, FEBS Lett. 582 (2008) 3625–3631.
[26] T.K. Ahn, T.J. Avenson, M. Ballottari, Y.C. Cheng, K.K. Niyogi, R. Bassi, G.R. Fleming, Architecture of a charge-transfer state regulating light harvesting in a plant antenna protein, Science 320 (2008) 794–797.
[27] A.V. Ruban, R. Berera, C. Ilioaia, I.H.M. van Stokkum, J.T.M. Kennis, A.A. Pascal, H. van Amerongen, B. Robert, P. Horton, R. van Grondelle, Identification of a mechanism of photoprotective energy dissipation in higher plants, Nature 450 (2007) 575–578.
[28] Z. Li, T.K. Ahn, T.J. Avenson, M. Ballottari, J.A. Cruz, D.M. Kramer, R. Bassi, G.R. Fleming, J.D. Keasling, K.K. Niyogi, Lutein accumulation in the absence of zeaxanthin restores nonphotochemical quenching in the *Arabidopsis thaliana* npq1 mutant, Plant Cell 21 (2009) 1798–1812.
[29] A. Dreuw, G. Fleming, M. Head-Gordon, Role of electron-transfer quenching of chlorophyll fluorescence by carotenoids in non-photochemical quenching of green plants, Biochem. Soc. Trans. 33 (2005) 858–862.
[30] R.N. Frese, M. Germano, F.L. de Weerd, I.H.M. van Stokkum, A.Y. Shkuropatov, V.A. Shuvalov, H.J. van Gorkom, R. van Grondelle, J.P. Dekker, Electric field effects on the chlorophylls, pheophytins, and beta-carotenes in the reaction center of photosystem II, Biochemistry 42 (2003) 9205–9213.
[31] R.N. Frese, M.A. Palacios, A. Azzizi, I.H.M. van Stokkum, J. Kruip, M. Rogner, N.V. Karapetyan, E. Schlodder, R. van Grondelle, J.P. Dekker, Electric field effects on red chlorophylls, beta-carotenes and P700 in cyanobacterial photosystem I complexes, Biochim. Biophys. Acta Bioenerg. 1554 (2002) 180–191.
[32] T. Nakabayashi, M. Wahadoszamen, N. Ohta, External electric field effects on state energy and photoexcitation dynamics of diphenylpolyenes, J. Am. Chem. Soc. 127 (2005) 7041–7052.
[33] L. Premvardhan, E. Papagiannakis, R.G. Hiller, R. van Grondelle, The charge-transfer character of the S-0 → S-2 transition in the carotenoid peridinin is revealed by stark spectroscopy, J. Phys. Chem. B 109 (2005) 15589–15597.
[34] M. Wahadoszamen, T. Harnada, T. Iimori, T. Nakabayashi, N. Ohta, External electric field effects on absorption, fluorescence, and phosphorescence spectra of diphenylpolyynes in a polymer film, J. Phys. Chem. A 111 (2007) 9544–9552.
[35] M. Wahadoszamen, T. Nakabayashi, S. Kang, H. Imahori, N. Ohta, External electric field effects on absorption and fluorescence spectra of a fullerene derivative and its mixture with zinc-tetraphenylporphyrin doped in a PMMA film, J. Phys. Chem. B 110 (2006) 20354–20361.
[36] A.M. Ara, T. Iimori, T. Nakabayashi, H. Maeda, K. Mizuno, N. Ohta, Electric field effects on absorption and fluorescence spectra of trimethylsilyl- and trimethylsilylethynyl-substituted compounds of pyrene in a PMMA film, J. Phys. Chem. B 111 (2007) 10687–10696.
[37] A.M. Ara, T. Iimori, T. Yoshizawa, T. Nakabayashi, N. Ohta, External electric field effects on fluorescence of pyrene butyric acid in a polymer film: concentration dependence and temperature dependence, J. Phys. Chem. B 110 (2006) 23669–23677.
[38] A.M. Ara, T. Iimori, T. Yoshizawa, T. Nakabayashi, N. Ohta, External electric field effects on fluorescence of perylene doped in a polymer film, Chem. Phys. Lett. 427 (2006) 322–328.
[39] E. Romero, M. Mozzo, I.H.M. van Stokkum, J.P. Dekker, R. van Grondelle, R. Croce, The origin of the low-energy form of photosystem I light-harvesting complex Lhca4: mixing of the lowest exciton with a charge-transfer state, Biophys. J. 96 (2009) L35–L37.
[40] A.V. Ruban, M.P. Johnson, C.D. Duffy, The photoprotective molecular switch in the photosystem II antenna, Biochim. Biophys. Acta Bioenerg. 1817 (2012) 167–181.
[41] X.-P. Li, O. BjoÈrkman, C. Shih, A.R. Grossman, M. Rosenquist, S. Jansson, K.K. Niyogi, A pigment-binding protein essential for regulation of photosynthetic light harvesting, Nature 403 (2000) 391–395.
[42] A.A. Pascal, Z. Liu, K. Broess, B. van Oort, H. van Amerongen, C. Wang, P. Horton, B. Robert, W. Chang, A. Ruban, Molecular basis of photoprotection and control of photosynthetic light-harvesting, Nature 436 (2005) 134–137.
[43] L. Dall'Osto, S. Caffarri, R. Bassi, A mechanism of nonphotochemical energy dissipation, independent from PsbS, revealed by a conformational change in the antenna protein CP26, Plant Cell 17 (2005) 1217–1232.
[44] A. Ruban, P. Horton, Mechanism of ΔpH-dependent dissipation of absorbed excitation energy by photosynthetic membranes. I. Spectroscopic analysis of isolated light-harvesting complexes, Biochim. Biophys. Acta Bioenerg. 1102 (1992) 30–38.
[45] M. Wahadoszamen, R. Berera, A.M. Ara, E. Romero, R. van Grondelle, Identification of two emitting sites in the dissipative state of the major light harvesting antenna, Phys. Chem. Chem. Phys. 14 (2012) 759–766.
[46] M. Wahadoszamen, A. Ghazaryan, H.E. Cingil, A.M. Ara, C. Büchel, R. van Grondelle, R. Berera, Stark fluorescence spectroscopy reveals two emitting sites in the dissipative state of FCP antennas, Biochim. Biophys. Acta Bioenerg. 1837 (2014) 193–200.
[47] M. Wahadoszamen, T. Nakabayashi, N. Ohta, Electroab sorption spectra of a complex formed between tetraphenyl-porphyrin and fullerene in a polymer film, J. Photochem. Photobiol. A Chem. 178 (2006) 177–184.
[48] M. Wahadoszamen, S. D'Haene, A.M. Ara, E. Romero, J.P. Dekker, R. van Grondelle, R. Berera, Identification of common motifs in the regulation of light harvesting: the case of cyanobacteria IsiA, Biochim. Biophys. Acta Bioenerg. 1847 (2015) 486–492.
[49] T.K. Ahn, T.J. Avenson, M. Ballottari, Y.-C. Cheng, K.K. Niyogi, R. Bassi, G.R. Fleming, Architecture of a charge-transfer state regulating light harvesting in a plant antenna protein, Science 320 (2008) 794–797.
[50] S. Amarie, L. Wilk, T. Barros, W. Kuhlbrandt, A. Dreuw, J. Wachtveitl, Properties of zeaxanthin and its radical cation bound to the minor light-harvesting complexes CP24, CP26 and CP29, Biochim. Biophys. Acta Bioenerg. 1787 (2009) 747–752.
[51] F. Passarini, E. Wientjes, R. Hienerwadel, R. Croce, Molecular basis of light harvesting and photoprotection in CP24 unique features of the most recent antenna complex, J. Biol. Chem. 284 (2009) 29536–29546.
[52] S. Amarie, J. Standfuss, T. Barros, W. Kühlbrandt, A. Dreuw, J. Wachtveitl, Carotenoid radical cations as a probe for the molecular mechanism of nonphotochemical quenching in oxygenic photosynthesis, J. Phys. Chem. B 111 (2007) 3481–3487.
[53] Y.-C. Cheng, T.K. Ahn, T.J. Avenson, D. Zigmantas, K.K. Niyogi, M. Ballottari, R. Bassi, G.R. Fleming, Kinetic modeling of charge-transfer quenching in the CP29 minor complex, J. Phys. Chem. B 112 (2008) 13418–13423.
[54] A.V. Ruban, A.J. Young, A.A. Pascal, P. Horton, The effects of illumination on the xanthophyll composition of the photosystem-ii light-harvesting complexes of spinach thylakoid membranes, Plant Physiol. 104 (1994) 227–234.
[55] A.V. Ruban, P.J. Lee, M. Wentworth, A.J. Young, P. Horton, Determination of the stoichiometry and strength of binding of xanthophylls to the photosystem II light harvesting complexes, J. Biol. Chem. 274 (1999) 10458–10465.
[56] R. Porra, W. Thompson, P. Kriedemann, Determination of accurate extinction coefficients and simultaneous equations for assaying chlorophylls a and b extracted with four different solvents: verification of the concentration of chlorophyll standards by atomic absorption spectroscopy, Biochim. Biophys. Acta Bioenerg. 975 (1989) 384–394.
[57] M. Wahadoszamen, I. Margalit, A.M. Ara, R. van Grondelle, D. Noy, The role of charge-transfer states in energy transfer and dissipation within natural and artificial bacteriochlorophyll proteins, Nat. Commun. 5 (2014).
[58] A. Moscatelli, K. Livingston, W.Y. So, S.J. Lee, U. Scherf, J. Wildeman, L.A. Peteanu, Electric-field-induced fluorescence quenching in polyfluorene, ladder-type polymers, and MEH-PPV evidence for field effects on internal conversion rates in the low concentration limit, J. Phys. Chem. B 114 (2010) 14430–14439.
[59] D.J. Lockhart, S.G. Boxer, Electric-field modulation of the fluorescence from *Rhodobacter-sphaeroides* reaction centers, Chem. Phys. Lett. 144 (1988) 243–250.
[60] K.A. Walters, D.A. Gaal, J.T. Hupp, Interfacial charge transfer and colloidal semiconductor dye-sensitization: mechanism assessment via stark emission spectroscopy, J. Phys. Chem. B 106 (2002) 5139–5142.
[61] V.I. Novoderezhkin, M.A. Palacios, H. van Amerongen, R. van Grondelle, Excitation dynamics in the LHCII complex of higher plants: modeling based on the 2.72 angstrom crystal structure, J. Phys. Chem. B 109 (2005) 10493–10504.
[62] D. Rutkauskas, J. Chmeliov, M. Johnson, A. Ruban, L. Valkunas, Exciton annihilation as a probe of the light-harvesting antenna transition into the photoprotective mode, Chem. Phys. 404 (2012) 123–128.
[63] W.F. Watson, R. Livingston, Concentration quenching of fluorescence in chlorophyll solutions, Nature 162 (1948) 452–453.
[64] G.S. Beddard, G. Porter, Concentration quenching in chlorophyll, Nature 260 (1976) 366–367.
[65] S.R. Marder, W.E. Torruellas, M. Blanchard-Desce, V. Ricci, G.I. Stegeman, S. Gilmour, J.-L. Brédas, J. Li, G.U. Bublitz, S.G. Boxer, Large molecular third-order optical nonlinearities in polarized carotenoids, Science 276 (1997) 1233–1236.
[66] V.I. Novoderezhkin, J.P. Dekker, R. van Grondelle, Mixing of exciton and charge-transfer states in photosystem II reaction centers: modeling of stark spectra with modified Redfield theory, Biophys. J. 93 (2007) 1293–1311.
[67] E. Wientjes, R. Croce, The light-harvesting complexes of higher-plant photosystem I: Lhca1/4 and Lhca2/3 form two red-emitting heterodimers, Biochem. J. 433 (2011) 477–485.
[68] V.I. Novoderezhkin, R. Croce, M. Wahadoszamen, I. Polukhina, E. Romero, R. van Grondelle, Mixing of exciton and charge-transfer states in light-harvesting complex Lhca4, Phys. Chem. Chem. Phys. 18 (2016) 19368–19377.